Heliyon 10 (2024) e29830

Contents lists available at ScienceDirect

Heliyon

journal homepage: www.cell.com/heliyon

Research article

Artificial multi-verse optimisation for predicting the effect of ideological and political theory course

Xingzhong Zhuang [a], Zhaodi Yi [a], Yuqing Wang [b], Yi Chen [c], Sudan Yu [d,*]

[a] College of Marxism, Wenzhou University, Wenzhou, 325035, China
[b] College of law, Wenzhou University, Wenzhou, 325035, China
[c] Department of Computer Science and Artificial Intelligence, Wenzhou University, Wenzhou, 325035, China
[d] Department of Artificial Intelligence, Wenzhou Polytechnic, Wenzhou, 325035, China

ARTICLE INFO

Keywords:
Teaching sufficiency
Artificial multi-verse optimizer
Classification
Art ideological and political theory course

ABSTRACT

Enhancing teaching sufficiency is crucial because low teaching efficiency has always been a widespread issue in ideological and political theory course. Evaluating data on the course is obtained from a freshmen class of 2022 using questionnaires. The data is organised and condensed for mining and analysis. Subsequently, an intelligent artificial multi-verse optimizer (AMVO) method s developed to predict the effect of ideological and political theory course. The proposed AMVO approach was tested against various cutting-edge algorithms to demonstrate its effectiveness and stability on the benchmark functions. The experimental results indicated that AMVO ranked first among the 23 test functions. Furthermore, the binary AMVO enhanced k-nearest neighbour classifier had excellent performance in the art ideological and political theory course in terms of error rate, accuracy, specificity and sensitivity. This model can predict the overall evaluation attitude of freshmen towards the course based on the dataset. In addition, we can further analyse the potential correlations between factors that enhance the intellectual and political content of the course. This model can further refine the evaluation of ideological and political courses by teachers and students in our school, thereby achieving the fundamental goal of moral cultivation.

1. Introduction

At the school's conference for instructors of ideological and political philosophy in 2019, the president of China delivered an important speech stating that 'the ideological and political theory course is the key course to implement the fundamental task of building morality and cultivating people' and discussed other important matters to encourage colleges and universities to innovate and update their course in political and ideological philosophy. To enhance the incorporation of art into the classroom, universities are introducing courses that encompass not only art forms but also explore ideological and political aspects. Among them, our school insists on establishing morality through aesthetic education; cultivating people by virtue; incorporating instruction in art aesthetic practice within the political and ideological framework of colleges and institutions; breaking through the 'island effect' that has long been dominated by ideological and political education, supplemented by other professional education; giving play to their respective

* Corresponding author.
E-mail addresses: zhuangxz@wzu.edu.cn (X. Zhuang), 00642006@wzu.edu.cn (Z. Yi), w13363215872@163.com (Y. Wang), kenyoncy2016@gmail.com (Y. Chen), yusudan07@sina.com (S. Yu).

https://doi.org/10.1016/j.heliyon.2024.e29830
Received 29 October 2023; Received in revised form 11 April 2024; Accepted 16 April 2024
Available online 17 April 2024

professional advantages; and establishing a long-term mechanism of coordinated development and education. However, colleges and universities find it challenging to understand the reform of the art ideological and political course, and a gap remains in the students' appraisal of the course. To strengthen the educational role of colleges and universities and help them elucidate the direction of future ideological and political course, it is necessary to conduct a thorough analysis of the evaluation of college students' participation in these courses.

In recent years, numerous scholars have conducted pertinent studies on the political and artistic courses offered at universities using big data. Based on the characteristics of instruction, He et al. proposed deep learning to formulate college students' ideological and political teaching strategies [1]. Lu introduced the practical and theoretical bases of the teaching method in a computer network environment [2]. In addition, Zhang et al. combined virtual reality (VR) technology with courses in universities and colleges and demonstrated that teaching in a VR classroom can promote students' understanding of knowledge while simulating their interests and establishing their emotional values and attitudes [3]. Li et al. employed the decision tree method as an example of machine learning to explore this theory course and made machine learning easier to understand in ideological and political course [4]. Furthermore, Yin et al. enhanced the incorporation of ideological and political aspects within microbiology experiments conducted at institutions of higher education, considering them as guiding principles for the development of ideological and political course [5]. Si developed a classification model for this course based on the SOM artificial network to forecast and host the professional courses [6].

In recent years, many intelligent optimisation algorithms (IOAs) inspired by natural phenomena have been developed, such as slime mould algorithm (SMA) [7], Harris Hawks Optimisation [8], Hunger Games Search (HGS) [9], Colony Predation Algorithm [10], Runge Kutta Optimizer (RUN) [11] and Weighted Mean of Vectors (INFO) [12]. Many fields have achieved remarkable success, such as medical diagnosis [13,14], optimisation of machine learning models [15] and multi-objective problems [16,17]. Numerous algorithms in the field include such as the Genghis Khan Shark Optimizer [18], Geyser Inspired Algorithm [19], Prairie Dog Optimisation Algorithm [20], Dwarf Mongoose Optimisation Algorithm [21], Gazelle Optimisation Algorithm [22], An Adaptive Hybrid Danlelion Optimizer (DETDO) [23], Firefly Algorithm [24], Artificial Hummingbird Algorithm [25].

In this research, we embark on an explorative journey through the intricate landscape of evolutionary computation frameworks and their profound applications in machine learning prediction. Central to our investigation are pioneering studies that not only demystify the underlying mechanisms but also pave the way for innovative methodologies within these realms. The generative model-based approach to evolutionary multi-objective search presented by Wang et al. [26] introduced a novel perspective on learning regularity, establishing a foundation for further exploration. Similarly, the work of Yi Chen and Aimin Zhou [27] on multi-objective portfolio optimisation via Pareto Front evolution exemplified the practical implications of evolutionary theories in optimizing complex systems. Further enriching this domain, Hao et al.'s study [28] enhanced surrogate-assisted evolutionary algorithms, offering a unique vantage point on leveraging unevaluated solutions for expensive optimisation challenges. Transitioning into the predictive capabilities enabled by machine learning, Li and Lin's hybrid ensemble QoS prediction approach [29], along with Chen et al.'s nonlinear combination method for wind speed prediction [30], illustrated the versatility and robustness of integrating diverse machine learning techniques. Additionally, Yang et al.'s contributions [31,32] underscored the significance of optimized machine learning frameworks in medical predictions, specifically addressing intradialytic hypotension using serum biomarkers and chronic kidney disease-related indexes. Together, these seminal works forged a cohesive narrative that not only enhanced our comprehension of evolutionary computation and machine learning predictions but also signals towards untapped potential awaiting discovery in these converging fields. Ultimately, we resorted to using the Multi-verse Optimizer (MVO) to predict the impact of ideological and political theory courses.

MVO, originally introduced by Mirjalili et al., in 2016, is a computational method [33]. MVO is an IOA with a simple structure inspired by the multi-verse theory. It dynamically updates each individual with its information and provides better individual information. Compared with other algorithms, MVO is characterised by a limited number of parameters and a delicate equilibrium between the exploration and exploitation strategies. In the research by Mirjalili et al., MVO showed better performance than other IOAs. Furthermore, numerous advanced MVO methods have been introduced and implemented across diverse domains. However, MVO has insufficient exploration capacity, leading to slow convergence speed and local optima. Therefore, we developed an artificial MVO (AMVO) that introduces the operator of the artificial bee colony (ABC) into MVO. The proposed model conducts a comprehensive analysis of the potential correlation between many parameters to enhance the content, structure and other aspects of the art's ideological and political path. Subsequently, it accurately predicts the dataset and achieves the core objective of promoting moral values and personal development.

This paper introduces an artificial mechanism to MVO algorithm, which is named AMVO. This method ranks first among the 23 classical function tests among other algorithms. The proposed binary AMVO (bAMVO) framework is used to train the k-nearest neighbour (KNN) model. The trained bAMVO-KNN model is substantiated for the first time to predict the effect of ideological and political theory course. This model was developed using questionnaires to collect evaluation data from the freshmen class of 2022. It was also employed to explore the key factors of the students' course. Compared with other machine learning methods, the developed bAMVO-KNN model exhibited an excellent performance in five evaluation indices, namely, classification accuracy (ACC), specificity, sensitivity, Matthews correlation coefficient (MCC) and error value.

The primary contributions of this study are as follows.

- An intelligent AMVO model is proposed for ideological and political theory course.
- History trajectory, diversity and balance analysis experiments show the global search capacity of AMVO.
- AMVO outperforms many other state-of-the-art methods in the function tests.
- The bAMVO-KNN model ranks first for feature selection on the datasets of ideological and political theory course, outperforming the others.

The main structure of the paper is organised as follows: Section 2 introduces the data collection and conventional algorithms. Section 3 proposes the AMVO method, the KNN model and the AMVO-KNN classifier. Section 4 discusses the experiment. Section 5 presents the discussion. Finally, Section 6 presents the conclusion of this paper.

2. Methods

2.1. Data collection and preparation

The primary source of data used in this study comprises students enrolled at various academic levels in Wenzhou University. The questionnaires were distributed to the students via WeChat. A total of 1300 copies were sent and 1266 were received, showing a response rate of 97 %. The 1266 students were included as research subjects, of whom 645 were from the liberal arts college, 463 from the science and engineering college, 120 from the arts college, 37 from the sports college and 1 from the national education college. Table 1 presents the 18 questions.

Table 1
Comprehensive delineation of the 18 questions.

Features	Name	Detailed description
f1	What is your college?	It is divided into five categories: liberal arts college, college of science and engineering, academy of art, physical culture institute and international college, which are represented by 1, 2, 3, 4 and 5, respectively.
f2	What is your gender?	Male and female students are represented by 0 and 1, respectively.
f3	What is your grade?	Levels 2022, 2021, 2020 and 2019
f4	How about the theme of the art ideological and political course? Is it clear and rich in content?	The major course of art, ideology and politics has a distinctive theme and rich content, with a score of 0–10.
f5	How is the duration appropriate for the emphasis of the art ideological and political course?	The key points of the art ideological and political course are highlighted, and the duration suitability is scored 0–10.
f6	Can the art ideological and political course combine the theme of the times and integrate the new elements of the present?	The art ideological and political course is scored 0–10, combining the theme of the times and integrating the new elements.
f7	How is the duration appropriate for the emphasis of the art ideological and political course?	The performance state and mental outlook of the actors in the art ideological and political course is scored 0–10.
f8	How smooth and complete is the chapter cohesion of the major art ideological and political course?	The smoothness and completeness of the discourse cohesion of the art, ideology and politics course are scored 0–10.
f9	Is the art ideological and political course in line with the strong artistic atmosphere and fully demonstrates the attitude of contemporary college students to strive for progress?	The artistic atmosphere of the art ideological and political course that shows the progressive life attitude of contemporary college students is scored 0–10.
f10	Does the art ideological and political course conform to the complete and rich programme planning and diversified display forms?	The programme planning of the art, ideology and politics course is complete and rich, and the diversity of display forms is scored 0–10.
f11	Can the art ideological and political course conform to the rhythm of the performance and is the programme arrangement of each chapter reasonable?	The rhythm of art ideological and political course is suitable, and the program arrangement of each chapter is reasonably divided into 0–10.
f12	How about your interest in art being improved through this course?	Students' interest in art is scored 0–10 after passing the art ideological and political course.
f13	How about your expression improved by the integration of ideology and politics with art through this major course?	The students understanding of the expression form of ideological and political integration and art through this art ideological and political course is scored 0–10.
f14	Does the art ideological and political course provide us with the correct aesthetic value orientation?	The major course of art ideology and politics provides us with the correct aesthetic value orientation, scoring 0–10.
f15	What is the most touching moment for me in this art ideological and political class?	According to the answers, 0 means no moving moments in the course and 1 means all moved. The touching moments are the speeches of the school leaders and representatives, the sense of ceremony, the spirit of the cast members, the performances, the audience's response, persistence, the atmosphere of the scene, feelings (patriotism, love the party, love the hometown, love the school) and others (stage effects, videos, hosts, staff, volunteers, etc.) in order to choose 2, 3, 4, 5, 6, 7 and 8, respectively.
f16	Which performers are the most popular?	My favourite program in this art ideological and political class is a flash song, I love Wen big, stand up, dragon, pond spring grass, strong state my youth, young, the moon, the light of faith, Kyushu and Tianyao China, navigator, which is represented by 1, 2, 3, 4, 5, 6, 7, 8.
f17	Would you like to join in the planning and performance of the art ideological and political class?	The willingness to participate in the planning and performance of art ideological and political course can be divided into very willing, willing and unwilling, which are represented by 1, 2 and 3, respectively.
f18	If I am one of the curators of the 2023 Art Ideology and Politics Course, what new forms and elements will I add?	According to the answers, the new forms and elements are classified into meaningless content, popular elements, scientific and technological elements, traditional cultural elements, language programmes, theme elements, ethnic elements, artistic elements and others, which are represented by 0, 1, 2, 3, 4, 5, 6, 7 and 8, respectively.

2.2. MVO

The fitness measure used by MVO is the expansion rate, whereby each universe is associated with a viable solution and the matter within each universe represents a variable. The quantity of universes is equivalent to the quantity of populations, whereas the quantity of matter within each universe serves as an indicator of the dimension of the problem. Under these rules, the MVO algorithm has two update mechanisms: a white/black hole tunnel and a wormhole tunnel. It is more probable that a universe characterised by a substantial pace of expansion will produce white holes. Conversely, it is more probable that a universe characterised by a low rate of expansion to give rise to black holes. There is a high probability of the formation of a white/black hole tunnel. Through the white/black hole tunnel, a universe with a higher expansion rate transfers matter into a universe with a lower expansion rate, thereby increasing the overall expansion rate. The white/black hole tunnel update method is a theoretical concept that is being discussed. The wheel selection mechanism identifies the universe that produces the white hole. Regardless of the effect of the expansion rate, a wormhole tunnel will be formed if a wormhole is present. At this point, the best universes can send matter through wormholes to other universes. In the wormhole tunnel update mechanism, wormholes appear with a particular random probability.

Assume $\overrightarrow{U}$ stands for the entire multi-verse; it includes n universes with d substances in each universe (i.e. the population size is denoted as n, whereas the dimension is represented by d), which is expressed as Eq. (1). $\overrightarrow{X}_i^j(t)$ shows the j th substance of the i th universe in the t th multi-verse. Eq. (2) simulates the white/black hole tunnel and Eq. (3) simulates the wormhole tunnel.

$$\overrightarrow{U}(t) = \begin{bmatrix} \overrightarrow{X}_1^1(t) & \overrightarrow{X}_1^2(t) & \cdots & \overrightarrow{X}_1^d(t) \\ \overrightarrow{X}_2^1(t) & \overrightarrow{X}_2^2(t) & \cdots & \overrightarrow{X}_2^d(t) \\ \vdots & \vdots & & \vdots \\ \overrightarrow{X}_n^1(t) & \overrightarrow{X}_n^2(t) & \cdots & \overrightarrow{X}_n^d(t) \end{bmatrix} \tag{1}$$

where r_1 denotes a stochastic number, which ranges from 0 to 1; $NI(\overrightarrow{X}_i(t))$, the normalisation of the expansion rate of all universes in a given t th generation; and $\overrightarrow{X}_k^j(t)$, the j th substance of the k th universe in the t th multi-verse. The roulette wheel selection mechanism [33] determines the white hole and matter sent out by the white hole.

$$\overrightarrow{X}_i^j(t+1) = \begin{cases} \overrightarrow{X}_k^j(t), & r_1 < NI\left(\overrightarrow{X}_i(t)\right) \\ \overrightarrow{X}_i^j(t), & r_1 \geq NI\left(\overrightarrow{X}_i(t)\right) \end{cases} \tag{2}$$

$$\overrightarrow{X}_i^j(t+1) = \begin{cases} \begin{cases} \overrightarrow{X}_{best}^j(t) + TDR \times ((ub - lb) \times r_4 + lb), & r_3 < 0.5 \\ \overrightarrow{X}_{best}^j(t) - TDR \times ((ub - lb) \times r_4 + lb), & r_3 \geq 0.5 \end{cases} & r_2 < WEP \\ \overrightarrow{X}_i^j(t), \quad r_2 \geq WEP \end{cases} \tag{3}$$

where $\overrightarrow{X}_{best}^j$ denotes the j th substance in the current best universe; ub and lb, the upper and lower bounds, respectively, representing the range of the variable; r_2,r_3,r_4, stochastic numbers ranging from zero to one; TDR, the travel distance rate; and WER, the wormhole existence rate. They are obtained using Eqs. (4) and (5).

$$WER = min + t \times \left(\frac{max - min}{T}\right) \tag{4}$$

$$TDR = 1 - \left(\frac{t^{1/p}}{T^{1/p}}\right) \tag{5}$$

where min and max denote the minimum and maximum values, T is the maximum iterations in advance and t is the current iteration value. In the original paper of MVO, p is defined as the exploitation accuracy over the iterations.

2.3. ABC method

The ABC method was introduced by Karaboga in 2005 [34], drawing inspiration from the foraging behaviour observed in natural bee colonies. ABC has four main components: lead bees, a food source, scout bees and follow bees. The quantity of the leading bees corresponds to the quantity of ideal solutions. The search method in ABC consists of three distinct steps.

(1) The foraging bees take on the role of leaders as they engage in search activity close to the identified food source. They then proceed to modify the location of the food in their memory, taking into account the distance of the food. If the candidate food exhibits a higher level of fitness than the original food source, it will upgrade. Otherwise, the position of the food is retained. This step is expressed as Eq. (6).

$$\vec{v}_i^j = \vec{X}_i^j + \vec{r}_i^j\left(\vec{X}_i^j - \vec{X}_k^j\right) \tag{6}$$

where $\vec{v}_i^j$ denotes the food source of the candidate, $\vec{r}_i^j$, a random parameter taking a value in the range of $[-1, 1]$ and $\vec{X}_k^j$, a randomly chosen solution k, which is not equal to i. After generating $\vec{v}_i^j$ inside the specified limits, the solution $\vec{v}_i^j$ can be assigned a fitness value for a minimisation problem by using Eq. (7).

$$fitness_i = \begin{cases} 1/((1+f_i)) if\, f_i \geq 0 \\ 1 + abs(f_i)\ if\ f_i\ <\ 0 \end{cases} \tag{7}$$

(2) After finding a food supply, the leading bees return to their dancing areas and swing their dances to alert the following bees about the availability of food. These bees use a roulette system to assess the size of the food source and decide whether to follow the leading bees in collecting honey. After comparing the fitness of the selected food source with that of the original food source, the following bees search their neighbourhoods using Eq. (6). The roulette wheel selection scheme, a fundamental component of the ABC method, uses a proportional allocation of slices based on the fitness value and is expressed as Eq. (8).

$$prob(i) = \frac{fitness_i}{\sum_{i=1}^{N} fitness_i} \tag{8}$$

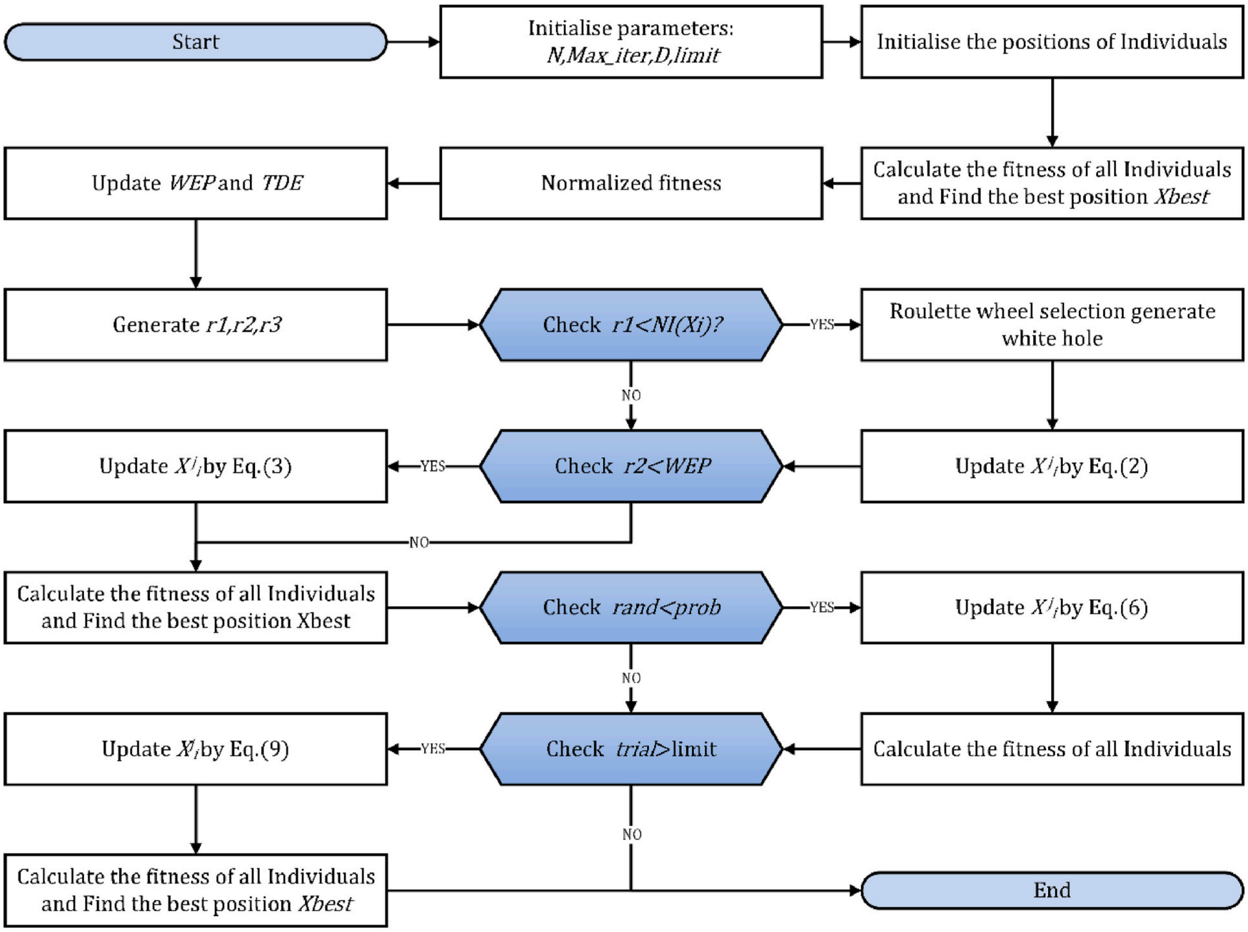

Fig. 1. Flowchart of AMVO

(3) When the food source location of the leading bees remains unchanged over multiple iterations, the food source location becomes trapped in local optima. The leading bee should give up its food source and become a scout bee. Thus, the original food source position is randomly replaced by an updated food source position. *rand* represents a random number between 0 and 1. The process of generating the new position for the food source is expressed as Eq. (9).

$$\overrightarrow{X}_i^j = \overrightarrow{X}_{max}^j + rand\left(\overrightarrow{X}_{max}^j - \overrightarrow{X}_{min}^j\right) \tag{9}$$

3. Proposed AMVO

This section presents an introduction to the pertinent concepts of the ABC and MVO algorithms. The operator of ABC is added to the MVO algorithm to improve its global search ability, which is further elaborated in the following part.

3.1. Proposed AMVO

In the proposed AMVO, the multi-verse completes its initialisation based on its means. To enhance the exploratory search capability of the original MVO, the multi-verse incorporates the foraging behaviour of the ABC to update its location. The foraging behaviour of artificial bees is expressed as Eqs. (6) and (9). The simplified pseudo-code of AMVO is presented in Algorithm 1, and the framework of AMVO is shown in Fig. 1.

Algorithm 1. Pseudo-code of AMVO

Begin
Initialise the parameters: T_{max}, Population size N, p;
Assess the overall fitness of the population and identify the most optimal individual;
While $t < T_{max}$
For i = 1:N
Compute the fitness and determine the best position X_{best};
Update WER using Equation (4);
Update TDR using Equation (5);
Normalise the fitness rate $NI(\overrightarrow{X}_i)$;
For each $\overrightarrow{X}_j^i$
Generate r_1, r_2, r_3.
If r_1 < NI $(\overrightarrow{\mathbf{X}}_\mathbf{i})$
Update $\overrightarrow{X}_i^j$ using Equation (2);
End if
If r_2 < WER
Update $\overrightarrow{X}_i^j$ using Equation (3);
End if
End for End For Update X_{best} and the best fitness
Update prob using Equation (8);
If rand < *prob*
Perform ABC strategy using Equation (6);
End if
Update X_{best} and the best fitness;
If trial > limit
Perform ABC strategy using Equation (9);
End if
Update X_{best}; $t = t + 1$;
End While
Terminate the loop and output the optimal fitness value and the corresponding solution X_{best} as the most optimal solution
End

Assuming the population size N, the dimension D and the iteration times T, we analyse the computational complexity of each part in detail. The computational complexity of MVO is determined by four critical factors: the max number of iteration, number of solution, the normalised sorting mechanism used to calculate the expansion rate and the roulette wheel selection mechanism employed to generate white holes. The sorting mechanism uses quicksort, of which the worst time complexity is $O(N^2)$.The time complexity of the roulette wheel selection mechanism is $O(logN)$.Therefore, the time complexity of MVO $is\, O(T * O(quick\ sort)$v $+ \ T * N * D * O(roulette\ wheel)) = O(T * N^2 + T * N * D * logN)$. Furthermore, the time complexity of ABC is $O(2 * N * D)$. Therefore, the entire complexity of AMVO is$O(T * N^2 + T * N * D * logN + T * 2 * N * D)$.

3.2. Classification based on KNN

The KNN algorithm [35] is a non-parametric and straightforward learning method that achieves impressive results in tasks involving function classification and approximation. It has been found to exhibit high completion rates and accurate classification, as reported by Zhu et al. [36–38]. The model used in this study is an instance-based learning approach, wherein the classification of an entirely fresh instance is determined based on the majority vote of the class labels of its KNN. By calculating the similarity between the new instance and the training point, the class associated with the nearest training point is selected to determine the classification of the new instance. The concept of similarity has been widely discussed in the academic literature, and the Euclidean distance is a commonly used metric for its measurement. The process for calculating the Euclidean distance between points Z_1 and Z_2 in the D-dimensional space is as Eq. (10).

$$Distance\ (Z_1, Z_2) = \sum_{i=1}^{D} \left(z_1^i - z_2^i\right) \tag{10}$$

Because of the fast speed, simple implementation and high efficiency of the KNN classifier, it has been used in this study to evaluate the classification ACC.

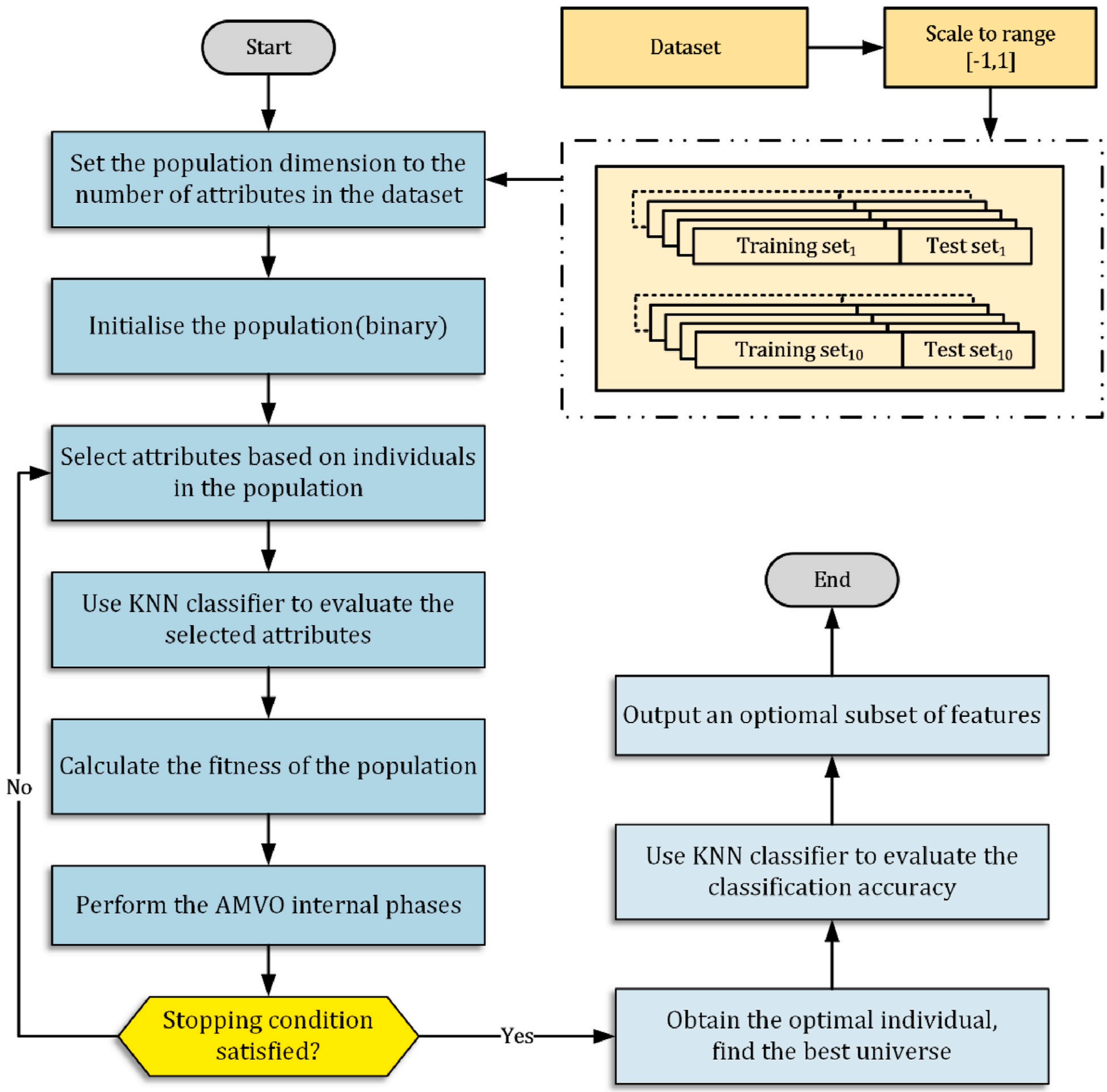

Fig. 2. Flowchart of the bAMVO-KNN model.

3.3. bAMVO-KNN model

To better classify the dataset, the combination of the bAMVO and KNN is utilised for feature selection. The aforementioned approach can yield findings that are easily understandable and can be effectively interpreted in the context of classification tasks. The processes of the model outlined in this research are presented in Algorithm 2, and the corresponding flowchart is depicted in Fig. 2.

Algorithm 2. Pseudo-code of bAMVO-KNN

Begin
The data are scaled to a range $[-1, 1]$ and divided into the test and training sets;
The population dimension is set to the number of attributes in the dataset;
Initialise the parameters: T_{max}, Population size N, p;
Assess the overall fitness of the population and identify the most optimal individual;
While $t < T_{max}$
For i $= 1{:}N$
Compute the fitness and determine the best position X_{best};
Update WER using Equation (4);
Update TDR using Equation (5);
Normalise the fitness rate $NI(\overrightarrow{X}_i)$;
For each $\overrightarrow{X}_j^i$
Generate r_1, r_2, r_3.
If $\mathbf{r_1} < NI\ (\overrightarrow{\mathbf{X}}_\mathbf{i})$
Update $\overrightarrow{X}_i^j$ using Equation (2);
End if
If $\mathbf{r_2}$ **< WER**
Update $\overrightarrow{X}_i^j$ using Equation (3);
End if
End for End For Transfer position in binary;
Use the KNN algorithm to evaluate the selected attributes;
Compute the current fitness;
Update X_{best}
Update prob using Equation (8);
If rand < *prob*
Perform ABC strategy using Equation (6);
End if
Transfer position in binary;
Use the KNN algorithm to evaluate the selected attributes;
Compute the current fitness;
Update X_{best};
If trial > limit
Perform ABC strategy using Equation (9);
End if
Transfer position in binary;
Use the KNN algorithm to evaluate the selected attributes;
Calculate the current fitness;
Update X_{best}; $t = t + 1$;
End While
Terminate the loop and output the optimal fitness value and corresponding solution X_{best} as the most optimal solution
End

Table 2
Descriptions of the unimodal functions.

Function expression	*Dim*	*Boundary*	$f_{\min}$
$F_1(x) = \sum_{i=1}^n x_i^2$	30	[−100, 100]	0
$F_2(x) = \sum_{i=1}^n \lvert x_i\rvert + \prod_{i=1}^n \lvert x_i\rvert$	30	[−10, 10]	0
$F_3(x) = \sum_{i=1}^n \left(\sum_{j-1}^i x_j\right)^2$	30	[−100, 100]	0
$F_4(x) = max_i\{\lvert x_i\rvert, 1 \le i \le n\}$	30	[−100, 100]	0
$F_5(x) = \sum_{i=1}^{n-1} [100(x_{i+1} - x_i^2)^2 + (x_i - 1)^2]$	30	[−30, 30]	0
$F_6(x) = \sum_{i=1}^n ([x_i + 0.5])^2$	30	[−100, 100]	0
$F_7(x) = \sum_{i=1}^n ix_i^4 + random[0, 1]$	30	[−128, 128]	0

4. Experiment and findings

4.1. Function optimisation validation

This study uses 23 benchmark functions as test sets to show the performance of the AMVO. The experimental design incorporated an array of test sets, which comprised a trio of function categories: seven unimodal functions designated as F1–F7, a quintet of multimodal functions labelled as F8–F12 and a suite of 11 multimodal benchmark functions with fixed dimensions, annotated as F14–F23. Tables 2–4 present a comprehensive compilation of the descriptions for the 23 benchmark routines. For a fair comparison, AMVO and other algorithms were assessed within the same set of settings. The study implemented a population size of 30 individuals and a maximum number of evaluations of 300,000. To mitigate potential confounding factors, the algorithms were subjected to 30 iterations of testing on the classical 23 benchmark functions. Within the scope of the study, the Friedman test was used as a non-parametric statistical procedure to ascertain and classify the performance metrics of various algorithms when applied to a benchmark function. This methodological approach enabled the systematic arrangement of algorithms based on their mean performance indices, thereby simplifying the subsequent execution of comparative statistical analyses and the articulation of average ranking figures. To enhance the clarity of data presentation within the tabulated outputs, the superior outcomes corresponding to each function have been accentuated using the bold typeface. The benchmark functions encompass a diverse range of highly intricate mathematical optimisation tasks. Thus, they are frequently used to assess the overall efficacy of algorithms. A statistical analysis of the average performance of all algorithms is conducted using the Friedman test, which allows for a comparison of their relative rankings.

The comparison algorithms comprise the Cloud Bat Algorithm (CBA) [39], Route Choice Behaviour Algorithm (RCBA) [40], Chaotic Fruit Fly Optimisation (CIFOA) [41], MVO, Sine Cosine Algorithm (SCA) [42–44], Moth-Flame Optimisation (MFO) [45–47] and Bat Algorithm (BA). These tests were written in MATLAB R2018b and implemented on a Microsoft Windows 11 platform equipped with a robust 16.0 GB of RAM and is powered by a 12th Generation Intel® Core™ i7-12700H CPU, which operates at a clock speed of 2.30 GHz.

All methodologies were assessed within the same set of settings to guarantee an impartial evaluation. To mitigate potential confounding factors, the algorithms were subjected to 30 iterations of testing on the benchmark functions. This paper presents the numerical results of the aforementioned approaches, which were selected based on the average (Avg.) and standard deviation (Std.) of the optimal function values. The average is used as a metric to assess the overall search capability, whereas the standard deviation is used to measure the resilience of the algorithm. Furthermore, the ideal outcomes for each problem are highlighted in bold to effectively show the optimal results. The statistical significance of the improvement was assessed using the Wilcoxon signed-rank test [48], a non-parametric test conducted at a significance level of 0.05. In the comparison of the proposed method with the other competitors in the proposed approach, the symbols '+', ' = ' and '−' were used to denote superiority, equality and inferiority, respectively.

The selection of the numerical results for these approaches was based on the Avg. and Std. of the optimal function values. Avg. is used to assess the overall search capability, whereas Std. is used to examine the resilience of the algorithm. Furthermore, the ideal outcomes for each problem are highlighted in bold to verify the global search capacity. The results of the AMVO algorithm and its 7 competitors on a set of 23 benchmark functions are presented in Table 5. The AMVO algorithm demonstrated optimal performance on several functions but did not exhibit the same level of optimisation as CIFOA on F1, F2, F3, F4, F9, F10 and F11; the disparity between the outcomes achieved by AMVO and the minimum values was minimal. In addition, AMVO achieves lower results than CBA and SCA on F6 and F5, respectively, but achieves optimal results on all benchmark functions. The utilisation of the operation for populations and people in AMVO can effectively mitigate the occurrence of local optima.

Table 6 presents the P-value derived from the use of the Wilcoxon signed-rank test. $P < 0.05$ was considered to indicate statistical significance. In the table, values that are below the threshold of 0.05 are written in black. The table shows that AMVO outperforms the other algorithms indicated across all 23 benchmark functions. While there are multiple P-values more than or equal to 0.05, the comparison of the outcomes between AMVO and the other mentioned methods does not exhibit significant differences. It is evident from the table that a majority of the data points are below the 0.05 threshold. Hence, it can be posited that AMVO exhibits superior

Table 3
Descriptions of the multimodal functions.

Function expression	*Dim*	Boundary	$f_{\min}$
$F_8(x) = \sum_{i=1}^{n} -x_i \sin(\sqrt{\lvert x_i \rvert})$	30	[−500, 500]	−418.9829 × 30
$F_9(x) = \sum_{i=1}^{n} [x_i^2 - 10\cos(2\pi x_i) + 10]$	30	[−5.12, 5.12]	0
$F_{10}(x) = -20\exp\left(-0.2\sqrt{\frac{1}{n}\sum_{i=1}^{n} x_i^2}\right) - \exp\left(\frac{1}{n}\sum_{i=1}^{n}\cos(2\pi x_i)\right) + 20 + e$	30	[−32, 32]	0
$F_{11}(x) = \frac{1}{4000}\sum_{i=1}^{n} x_i^2 - \prod_{i=1}^{n}\cos\left(\frac{x_i}{\sqrt{i}}\right) + 1$	30	[−600, 600]	0
$F_{12}(x) = \frac{\pi}{n}\{10\sin(\pi y_1) + \sum_{i=1}^{n-1}(y_i - 1)^2[1 + 10\sin^2(\pi y_{i+1})] + (y_n - 1)^2\} + \sum_{i=1}^{n} u(x_i, 10, 100, 4)\ y_i = 1 + \frac{x_i + 1}{4}$ $u(x_i, a, k, m) = \begin{cases} k(x_i - a)^m & x_i > a \\ 0 & -a < x_i < a \\ k(-x_i - a)^m & x_i < -a \end{cases}$	30	[−50, 50]	0
$F_{13}(x) = 0.1\{\sin^2(3\pi x_1) + \sum_{i=1}^{n}(x_i - 1)^2[1 + \sin^2(3\pi x_i + 1)] + (x_n - 1)^2[1 + \sin^2(2\pi x_n)]\} + \sum_{i=1}^{n} u(x_i, 5, 100, 4)$	30	[−50, 50]	0

Table 4
Expositions on the multimodal functions of invariant dimensions.

Function expression	*Dim*	Boundary	$f_{\min}$
$F_{14}(x) = \left(\frac{1}{500} + \sum_{j=1}^{25} \frac{1}{j + \sum_{i=1}^{2}(x_i - a_{ij})^6}\right)^{-1}$	2	[−65, 65]	1
$F_{15}(x) = \sum_{i=1}^{11} \left[a_i - \frac{x_1(b_i^2 - b_i x_2)}{b_i^2 + b_i x_3 + x_4}\right]^2$	4	[−5, 5]	0.00030
$F_{16}(x) = 4x_1^2 - 2.1x_1^4 + \frac{1}{3}x_1^6 + x_1x_2 - 4x_2^2 + 4x_2^4$	2	[−5, 5]	−1.0316
$F_{17}(x) = \left(x_2 - \frac{5.1}{4\pi^2}x_1^2 + \frac{5}{\pi}x_1 - 6\right)^2 + 10\left(1 - \frac{1}{8\pi}\right)\cos x_1 + 10$	2	[−5, 5]	0.398
$F_{18}(x) = [1 + (x_1 + x_2 + 1)^2(19 - 14x_1 + 3x_1^2 - 14x_2 + 6x_1x_2 + 3x_2^2)] \times [30 + (2x_1 - 3x_2)^2 \times (18 - 32x_1 + 12x_1^2 + 48x_2 - 36x_1x_2 + 27x_2^2)]$	2	[−2, 2]	3
$F_{19}(x) = -\sum_{i=1}^{4} c_i \exp(-\sum_{j=1}^{3} a_{ij}(x_j - p_{ij}])^2)$	3	[1,3]	−3.86
$F_{20}(x) = -\sum_{i=1}^{4} c_i \exp(-\sum_{j=1}^{6} a_{ij}(x_j - p_{ij}])^2)$	6	[0, 1]	−3.32
$F_{21}(x) = -\sum_{i=1}^{5} [(X - a_i)(X - a_i)^T + c_i]^{-1}$	4	[0, 10]	−10.1532
$F_{22}(x) = -\sum_{i=1}^{7} [(X - a_i)(X - a_i)^T + c_i]^{-1}$	4	[0, 10]	−10.4028
$F_{23}(x) = -\sum_{i=1}^{10} [(X - a_i)(X - a_i)^T + c_i]^{-1}$	4	[0, 10]	−10.5363

outcomes compared with the other seven methods.

Fig. 3 presents the convergence effect of the AMVO algorithm on various benchmark test functions, namely, F8, F12, F13, F14, F20 and F22. The convergence curves are derived from the evaluation process through the sequential selection of 50 data points, which are subsequently plotted as continuous curves. The image shows that AMVO exhibits both the lowest convergence rate and the highest convergence speed across the functions. The convergence image clearly shows that the AMVO algorithm exhibits significant enhancements in both population diversity and convergence accuracy compared with the basic MVO algorithm.

4.2. History trajectory

In this section, the AMVO employs historical trajectory of multiple functions to evaluate the impact of global and local exploitation searches [49,50]. Fig. 4 presents the temporal evolution of 3 archetypes over 23 benchmark functions across 1000 iterations, including 2 unimodal benchmark test functions F1 and F5, 2 multimodal benchmark test functions F8 and F9 and 2 fixed-dimension multimodal benchmarks F14 and F22. The red line indicates AMVO, whereas the other blue line represents MVO. Fig. 4(a) demonstrates the graphical plots of the selected mathematical formulas based on AMVO. Fig. 4(b) presents a graphical representation of the historical search trajectory executed by the agents of the AMVO algorithm, targeting the optimal solution within the designated search space throughout 1000 iterations, as applied to the specified functions. The trajectory acquired by AMVO iterating in the first dimension is depicted in Fig. 4(c). Fig. 4 shows that AMVO is volatile in the early period but becomes stable in the later stage. Thus, there is a strong likelihood of the population dispersing around the ideal position. The average fitness of iterative agents is presented in Fig. 4(d), which indicates that the average distance variation of the AMVO population is larger than that of MVO and that the search for space is more adequate. Fig. 4(e) shows the function fitness curve calculated by AMVO and MVO. AMVO quickly converges to the final optimized minimum value.

Briefly, history trajectory diagrams for six representative functions, F1, F5, F8, F9, F14 and F22 are provided. Fig. 4 displays a graphical plot and analyses the search history of AMVO for the different functions. Comparisons of the agent trajectory, average fitness among all agents and converging curves in AMVO and MVO are depicted in Fig. 4. Ultimately, AMVO performs well in unimodal, multimodal and fixed-dimension multimodal benchmarks compared with MVO.

4.3. Balance and diversity analysis

In this section, a deeper analysis of the exploration and exploitation balances of AMVO and MVO will help us understand why global optimisation cases exhibit an outstanding performance. Fig. 5 presents the balance analysis of AMVO and MVO and their diversity analysis. Balance and diversity analysis are conducted on 6 functions selected from 23 benchmark functions, namely, F1, F2, F8, F9, F14 and F16.

As can be seen from Fig. 5, the balance analysis of AMVO and MVO shows exploration, exploitation and incremental–decremental curves. The red lines indicate the global exploration searches, whereas the blue curves represent the local exploitation searches. The incremental–decremental curve is indicated by green lines. The proportion of AMVO of the global exploration searches is greater than that of MVO due to the additional mechanism. The green curve indicates an upwards tendency if the exploratory search is greater than the exploitation search. A decreasing trend is observed when the magnitude of the exploratory search does not exceed that of the exploitative search. The low or high iteration values in the figure over time indicate the lasting results of either local exploitation or global exploration in the search method, respectively. Evaluation of AMVO in terms of F1, F2, F8, F9, F14 and F16, which include a

Table 5
Comparison of the optimal values obtained by AMVO with famous IOAs.

	Item	AMVO	CBA	RCBA	CIFOA	MVO	SCA	MFO	BA
F1	Avg	1.72266E−04	5.30042E−09	9.07526E−03	**0.00000E+00**	3.03182E−03	3.60944E−56	2.00000E+03	5.54056E−01
	Std	1.68256E−04	1.56570E−08	2.75576E−03	**0.00000E+00**	7.40122E−04	1.70073E−55	4.06838E+03	3.22643E−01
F2	Avg	5.31596E−03	2.08087E+01	5.35463E−01	**0.00000E+00**	4.11935E−02	3.12387E−58	3.33333E+01	3.30560E+00
	Std	2.06448E−03	3.77634E+01	1.15032E−01	**0.00000E+00**	1.14124E−02	1.62328E−57	2.35377E+01	1.31049E+00
F3	Avg	1.37283E+00	1.43487E+01	2.18367E+00	**0.00000E+00**	4.08149E−01	5.78382E+00	2.10000E+04	2.84310E−01
	Std	6.94450E−01	6.84308E+00	7.44997E−01	**0.00000E+00**	1.98994E−01	2.20846E+01	1.43145E+04	3.10297E−01
F4	Avg	1.87329E−01	8.41264E+00	2.20710E−01	**0.00000E+00**	9.10788E−02	9.42846E−03	5.86366E+01	5.99832E+00
	Std	6.68463E−02	8.49368E+00	8.04259E−02	**0.00000E+00**	3.78179E−02	4.55364E−02	1.17616E+01	5.18235E+00
F5	Avg	3.92996E+01	7.90305E+01	4.45172E+01	2.87221E+01	1.80051E+02	**2.73850E+01**	1.82622E+04	2.38052E+02
	Std	3.98435E+01	1.58872E+02	5.59462E+01	**1.71344E−01**	2.58394E+02	6.62833E−01	3.64934E+04	4.59254E+02
F6	Avg	9.06594E−05	**1.02062E−08**	8.96892E−03	6.76871E+00	3.27467E−03	3.65116E+00	2.34339E+03	5.01458E−01
	Std	6.73647E−05	**5.07220E−08**	2.33807E−03	1.15947E−01	7.36555E−04	1.85337E−01	5.05607E+03	3.03654E−01
F7	Avg	**3.08409E−03**	8.11673E−02	1.24081E−01	8.76663E−05	3.26060E−03	2.45153E−03	3.56487E+00	1.50642E+01
	Std	**1.00189E−03**	1.61048E−01	4.47926E−02	5.67423E−05	1.05525E−03	2.97282E−03	6.53180E+00	1.03542E+01
F8	Avg	**−1.00358E+04**	−7.41531E+03	−7.18938E+03	−2.76426E+03	−8.25018E+03	−4.38238E+03	−8.86651E+03	−7.19856E+03
	Std	5.17927E+02	6.86354E+02	7.50080E+02	1.06633E+03	7.20329E+02	**2.58811E+02**	9.70834E+02	7.35235E+02
F9	Avg	2.36470E+01	1.20517E+02	1.94235E+01	**0.00000E+00**	8.47720E+01	1.99700E+00	1.62921E+02	2.52028E+02
	Std	1.30086E+01	3.35491E+01	4.33712E+00	**0.00000E+00**	1.82159E+01	7.89011E+00	3.97402E+01	2.11285E+01
F10	Avg	2.77968E−03	1.47479E+01	1.19131E−01	8.88178E−16	5.77222E−02	1.28343E+01	1.23236E+01	2.57766E+00
	Std	1.22235E−03	2.70621E+00	3.91880E−02	**0.00000E+00**	2.42368E−01	8.47413E+00	9.05242E+00	3.36287E+00
F11	Avg	2.82260E−02	1.41240E−02	1.24336E−02	**0.00000E+00**	2.56949E−02	**0.00000E+00**	2.11170E+01	1.00189E−02
	Std	2.71222E−02	1.95296E−02	1.19319E−02	**0.00000E+00**	1.07233E−02	**0.00000E+00**	5.65526E+01	1.22153E−02
F12	Avg	**2.07768E−06**	1.55390E+01	8.36420E+00	8.16337E−01	1.01839E−01	3.68189E−01	1.94067E−01	6.94167E+00
	Std	**3.00899E−06**	7.15073E+00	2.83276E+00	3.63069E−02	2.71166E−01	1.03391E−01	3.85355E−01	2.95173E+00
F13	Avg	**1.62230E−05**	2.70631E+01	4.18392E−03	2.58014E+00	3.64864E−03	2.00047E+00	1.51378E−01	1.52886E−01
	Std	**1.44329E−05**	2.87272E+01	3.62591E−03	4.37835E−02	5.16345E−03	1.33234E−01	4.40430E−01	9.47466E−02
F14	Avg	**9.98004E−01**	1.69067E+00	8.44642E+00	1.14387E+01	**9.98004E−01**	**9.98004E−01**	1.98680E+00	3.04041E+00
	Std	**6.11252E−14**	1.35234E+00	7.25998E+00	3.31109E+00	3.13080E−13	5.20107E−07	1.63627E+00	1.96728E+00
F15	Avg	**3.77851E−03**	4.68437E−03	5.33404E−03	6.59216E−04	5.02091E−03	7.01471E−04	1.31918E−03	6.72967E−03
	Std	**7.38996E−03**	7.98124E−03	8.43661E−03	1.17798E−04	8.61037E−03	4.40979E−04	1.41393E−03	9.08073E−03
F16	Avg	**−1.03163E+00**	**−1.03163E+00**	**−1.03163E+00**	−4.79577E−01	**−1.03163E+00**	**−1.03163E+00**	**−1.03163E+00**	**−1.03153E+00**
	Std	5.63683E−10	5.05780E−07	1.33401E−08	1.55676E−01	2.89816E−09	1.32582E−06	**6.77522E−16**	8.27799E−05
F17	Avg	**3.97887E−01**	**3.97888E−01**	**3.97887E−01**	1.10331E+01	**3.97887E−01**	**3.98030E−01**	**3.97887E−01**	**3.97951E−01**
	Std	1.13013E−09	5.23844E−07	1.35106E−08	1.39365E+01	3.73379E−09	1.66386E−04	**0.00000E+00**	5.23874E−05
F18	Avg	3.00000E+00	**3.00002E+00**	**3.00000E+00**	1.53488E+02	**3.00000E+00**	**3.00000E+00**	**3.00000E+00**	3.00748E+00
	Std	7.83519E−09	4.29188E−05	5.65936E−07	1.71050E+02	1.96397E−08	2.11515E−07	1.52058E−15	8.36110E−03
F19	Avg	**−3.86278E+00**	**−3.86277E+00**	**−3.86278E+00**	−2.77695E+00	**−3.86278E+00**	−3.85485E+00	**−3.86278E+00**	−3.85363E+00
	Std	2.81308E−09	3.24575E−05	6.68995E−06	9.77337E−01	6.20193E−09	5.27105E−05	**2.71009E−15**	3.35323E−03
F20	Avg	**−3.26255E+00**	**−3.26035E+00**	**−3.25836E+00**	−1.39033E+00	**−3.25858E+00**	−2.96624E+00	−3.22270E+00	−3.01693E+00
	Std	6.04628E−02	6.20398E−02	6.04933E−02	5.55166E−01	**6.03321E−02**	3.05271E−01	9.55213E−02	7.44038E−02
F21	Avg	**−7.95774E+00**	−5.70596E+00	−7.88519E+00	−7.96229E−01	−8.12463E+00	−2.22605E+00	−7.06000E+00	−7.77902E+00
	Std	**2.55356E+00**	2.91875E+00	2.90779E+00	4.82708E−01	2.52699E+00	**2.29109E+00**	3.45872E+00	2.32035E+00
F22	Avg	**−1.00513E+01**	−6.02247E+00	−9.36636E+00	−9.49034E−01	−9.69835E+00	−4.77592E+00	−8.31745E+00	−8.46333E+00
	Std	**1.33809E+00**	3.70933E+00	2.40591E+00	4.67658E−01	1.82707E+00	2.80687E+00	3.26676E+00	2.03509E+00
F23	Avg	**−9.63823E+00**	−5.85636E+00	−9.03088E+00	−1.17236E+00	**−9.63980E+00**	−5.99401E+00	−7.86724E+00	−8.77997E+00
	Std	2.04274E+00	3.91460E+00	3.09494E+00	5.85248E−01	2.03917E+00	**1.83534E+00**	3.58348E+00	2.01487E+00
+/−/ =		~	16/3/4	17/1/5	13/8/2	15/3/5	15/6/2	9/4/10	20/2/1
Avg		**2.522**	5.435	4.609	4.783	3.304	4.478	5.087	5.739
Rank		**1**	7	4	5	2	3	6	8

Table 6
P-value was obtained using the Wilcoxon signed-rank test to compare the performances between AMVO and other algorithms.

	CBA	RCBA	CIFOA	MVO	SCA	MFO	BA
F1	**0.0000017**	**0.0000017**	**0.0000017**	**0.0000017**	**0.0000017**	**0.165027**	**0.0000017**
F2	**0.0000017**	**0.0000017**	**0.0000017**	**0.0000017**	**0.0000017**	**0.0000024**	**0.0000017**
F3	**0.0000017**	**0.000261**	**0.0000017**	**0.0000039**	**0.003379**	**0.0000032**	**0.0000058**
F4	**0.0000017**	0.071903	**0.0000017**	**0.0000077**	**0.0000019**	**0.0000017**	**0.0000035**
F5	0.360039	0.861213	0.205888	**0.0087300**	0.205888	**0.025637**	**0.000359**
F6	**0.0000017**	**0.0000017**	**0.0000017**	**0.0000017**	**0.0000017**	0.165027	**0.0000017**
F7	**0.0000017**	**0.0000017**	**0.0000017**	0.585712	**0.007731**	**0.0000017**	**0.0000017**
F8	**0.0000017**	**0.0000017**	**0.0000017**	**0.0000026**	**0.0000017**	**0.0000407**	**0.0000017**
F9	**0.0000017**	**0.262299**	**0.0000017**	**0.0000017**	**0.0000197**	**0.0000017**	**0.0000017**
F10	**0.0000017**	**0.0000017**	**0.0000017**	**0.0000017**	**0.0000077**	**0.0000531**	**0.0000017**
F11	**0.027029**	**0.009271**	**0.0000017**	0.813017	**0.0000017**	0.477947	**0.004682**
F12	**0.0000017**	**0.0000017**	**0.0000017**	**0.0000017**	**0.0000017**	0.102011	**0.0000017**
F13	**0.0000047**	**0.0000017**	**0.0000017**	**0.0000017**	**0.0000017**	**0.003609**	**0.0000017**
F14	0.503833	**0.0000047**	**0.0000017**	**0.0002410**	**0.0000017**	0.102011	**0.0000017**
F15	0.068714	0.075213	0.628843	0.465283	0.643517	0.440522	**0.006035**
F16	**0.0000085**	**0.0000149**	**0.0000017**	**0.0000063**	**0.0000017**	**0.0000017**	**0.0000017**
F17	**0.001833**	**0.001833**	**0.0000017**	**0.0000579**	**0.0000017**	**0.0000017**	**0.0000017**
F18	**0.0000019**	**0.0000019**	**0.0000017**	**0.000332**	**0.0000751**	**0.0000017**	**0.0000017**
F19	**0.0000047**	**0.0000017**	**0.0000017**	**0.0000024**	**0.0000017**	**0.0000017**	**0.0000017**
F20	0.106394	**0.040702**	**0.0000017**	0.068714	**0.0000017**	**0.0000017**	**0.0000017**
F21	**0.000616**	0.338856	**0.0000017**	**0.503833**	**0.0000032**	0.718888	0.205888
F22	**0.0000085**	**0.0000022**	**0.0000017**	**0.000205**	**0.0000017**	0.991795	**0.000115**
F23	**0.0000149**	**0.013975**	**0.0000017**	**0.009271**	**0.0000012**	0.452807	**0.011748**

greater exploration fraction than MVO, shows the breadth and depth of the worldwide exploration effects of AMVO.

The diversity analysis of F1, F2, F8, F9, F14 and F16 is demonstrated in the last line of Fig. 5. The x-axis represents the number of iterations, whereas the y-axis indicates the diversity measure. Random initialisation ensures that algorithms always begin with a large deal of diversity, and population diversity progressively declines as the number of iterations increases. The results indicate that the diversity values of AMVO decline are faster and smaller than those of MVO.

4.4. Feature selection experiment in the collected dataset

The efficiency of the proposed bAMVO-KNN method is tested by comparing it with other machine learning techniques, including the bMVO-KNN, bWOA-KNN, bSMA-KNN, bHGS-KNN, bDE-KNN and bRUN-KNN classification models. The specific algorithms contain the whale optimisation algorithm [51], SMA, HGS, differential evolution [52] and RUN.

Convention is used to set the parameters of the remaining classifiers. The accuracy of the classification is evaluated using an unbiased 10-fold cross-validation (CV) test. A subset of the data from the dataset is used as a test set, whereas the remaining data is used as a training set for the classifier. The validation number of each dataset is equal to the number of test datasets. The classification task is accomplished using the KNN classifier. The field size k is equal to 1 for KNN.

To be fair, the mentioned algorithms are run in one main function. For each method, the same main function has the same random initialisation. The number of search agents is 20, the fold is 10 times and the maximum number of evaluations is 50 in the same experimental environment. Furthermore, to assess the effectiveness of bAMVO-KNN, we use four widely recognised measures, namely, specificity, sensitivity, classification ACC and MCC.

The effectiveness of the classifier is verified by four mutual rules derived from the confusion matrix. Four predominant metrics, extrapolated from the confusion matrix, are used to quantify the efficacy of the proffered binary classification model in predictive analysis. These metrics are defined as follows.

1) The concordance between positive prediction and positive actuality is denoted as true positive.
2) The alignment of negative prediction with negative reality is indicated as true negative.
3) The discrepancy where a positive prediction contradicts a negative actuality is characterised as false positive.
4) The divergence wherein a negative prediction contrasts with a positive actuality is identified as false negative.

In this study, we provide Eqs. (11)–(14) to restrict the discourse within the boundaries of our research:

$$Accuracy = \frac{TP + TN}{TP + TN + FP + FN} \tag{11}$$

$$Specificity = \frac{TN}{FP + TN} \tag{12}$$

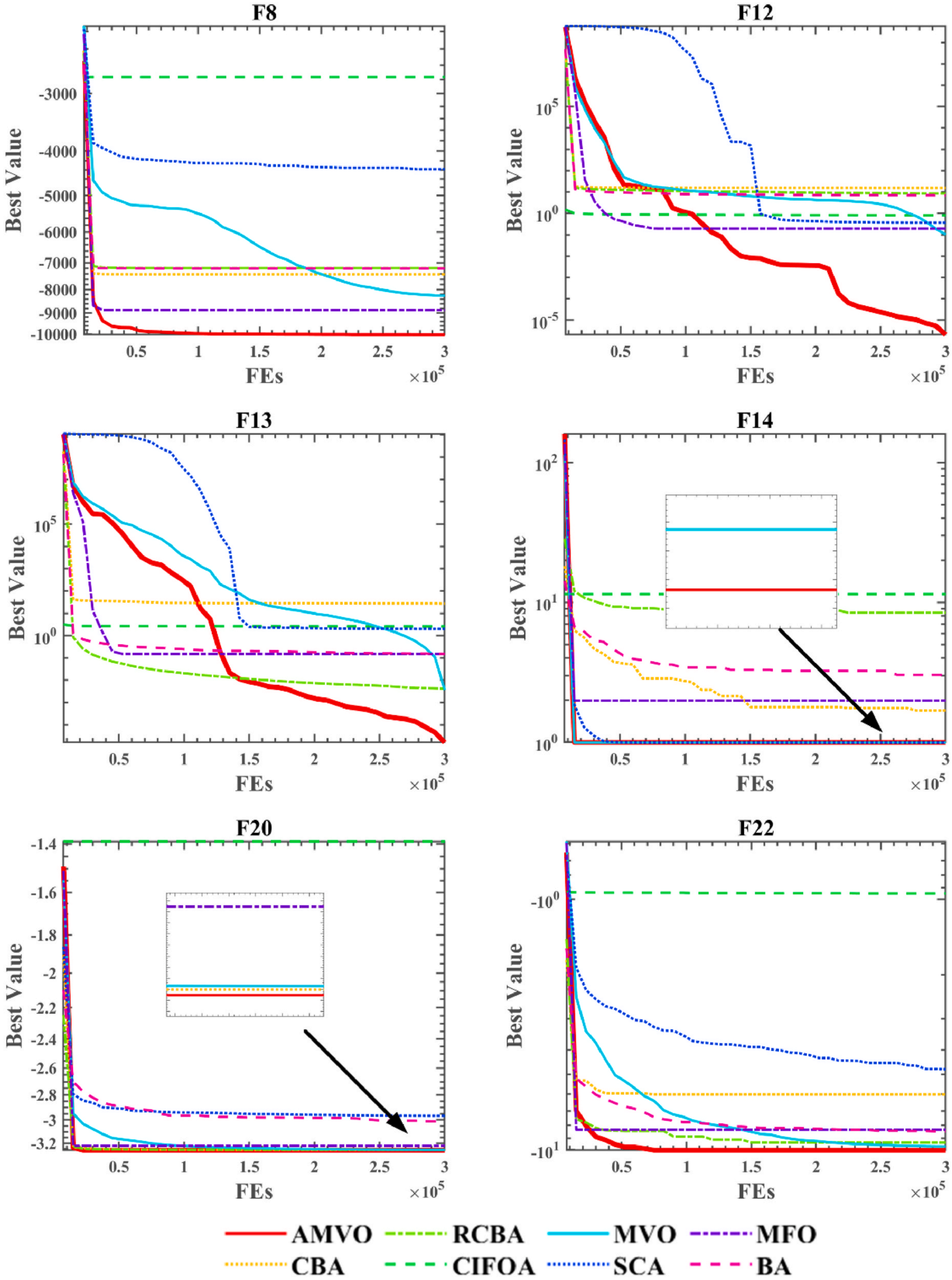

Fig. 3. Convergence trajectories of AMVO in comparison with other IOAs for six functions.

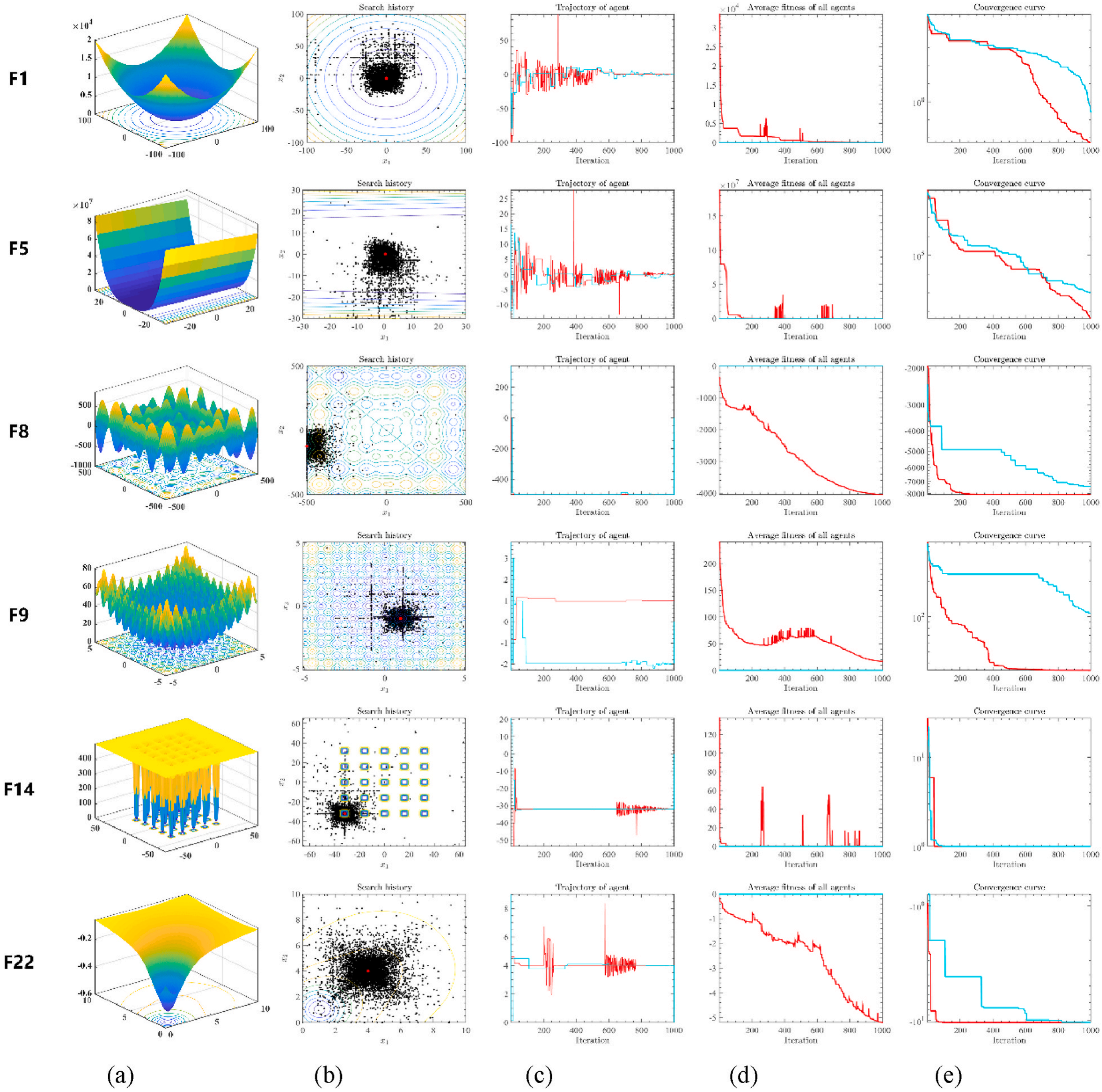

Fig. 4. Historical trajectory.

$$Sensitivity = \frac{TP}{TP + FN} \tag{13}$$

$$MCC = \frac{TP \times TN - FP \times FN}{\sqrt{(TP + FP) \times (TP + FN) \times (TN + FP) \times (TN + FN)}} \tag{14}$$

Feature selection is governed by two antithetical principal objectives: minimisation of the feature subset cardinality and maximisation of classification precision. An inverse correlation is frequently observed, wherein an augmentation in the classification ACC corresponds to a reduction in the number of selected features, thereby denoting an enhanced efficacy of classification. Throughout the iterative processes, a fitness function is commonly used to evaluate the merit of individual solutions. In the culmination of this process, bAMVO-KNN demonstrates proficiency in equilibrating classification precision with the parsimony of feature selection. The derived adaptive function is subsequently delineated as Eq. (15).

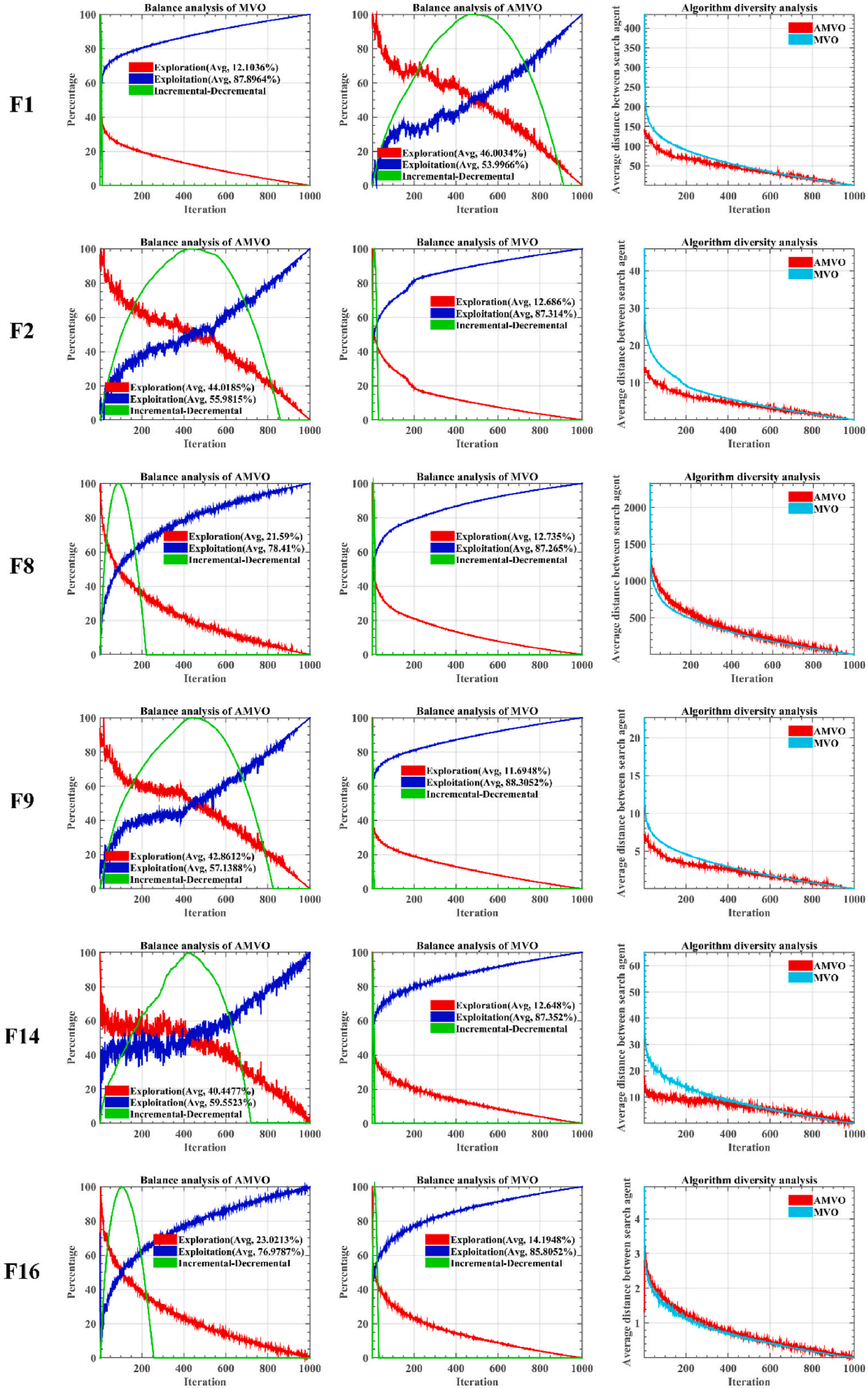

Fig. 5. Balance and diversity analyses of AMVO and MVO.

$$Fitness = \alpha \bullet \gamma_R(\mathrm{D}) + \beta \frac{|R|}{|N|} \quad (15)$$

where α denotes the weight of the classification ACC in the range of [0, 1]; γ_R, the classification error rate; $\beta = 1 - \alpha$, the criticality of the number of selected features; $|R|$, the size of the subset of the selected features; and $|N|$, the total number of all features. After many tests, the best effect is obtained under the condition of $\alpha = 0.05$ [53].

To evaluate the efficacy of feature selection, the proposed bAMVO-KNN model is compared with other commonly used techniques that rely on the KNN classifier for feature selection. The results of the Wilcoxon signed-rank test presented in Table 7 indicate that bAMVO-KNN is better than the other algorithms in terms of the ACC, sensitivity, specificity, MCC and error rate. Although the time cost of the proposed model ranks fifth, it is smaller than that of the original MVO. This shows that the time consumption does not increase when the ABC mechanism is added to MVO. The time consumption of AMVO is 5.6, which is within the acceptable range. The test results indicate that bAMVO-KNN can handle the classification of the collected dataset and can provide some help for teachers in practice.

Table 8 presents the outcomes of the feature selection executed by the bAMVO-KNN model, encompassing various parameters such as fold number, dimensionality of the selected feature subset and performance metrics, namely, classification ACC, sensitivity, specificity and MCC. The results indicate that the bAMVO-KNN model achieves a commendable ACC of 99.6 %, sensitivity of 100 %, specificity of 99.18 % and MCC of 99.26 %.

Finally, the features selected by bAMVO-KNN model from 10-fold CV test are calculated to analyse the classification results. The number of selected features is presented in Fig. 6. As can be seen from Fig. 6, the frequently selected features influence the expression form of students' art ideological and political course, actors' performance status, subject content and the theme of the times. Further analysis reveals the significance of these four features. Therefore, the bAMVO-KNN model can help teachers analyse the crucial factors and provide accurate classification results.

5. Discussion

In this study, AMVO ranks first on 23 benchmark functions among the other algorithms, namely, CBA, RCBA, CIFOA, MVO, SCA, MFO and BA. The history trajectory functions show the influence of the global and local search ability of AMVO, and the balance analysis reveals the breadth and depth of its worldwide exploration. The diversity analysis also reveals that the values gained by AMVO decreases faster than CBA, RCBA, CIFOA, MVO, SCA, MFO and BA. Compared with bMVO-KNN, bWOA-KNN, bSMA-KNN, bHGS-KNN, bDE-KNN and bRUN-KNN, bAMVO-KNN, which is based on the KNN model, performs the best in predicting the effect of ideological and political theory course. Although the computation time efficiency is not good, the bAMVO-KNN model is expected to discern the quintessential feature subset from datasets about ideological and political theory course, thereby ensuring superior accuracy, sensitivity, specificity and MCC and minimisation of classification error rate while retaining salient features. This outcome substantiates that the artificial strategy predicated on MVO underwrites enhancements in the scope of global exploration, thus facilitating a more adept equilibrium between local exploitation and broad-spectrum exploratory processes. Consequently, the empirical data for the proposed bAMVO-KNN model surpass that of other methodologies included in this study.

It is imperative to deeply analyse the evaluation of college students' participation in the major courses of art ideology and politics, which will help colleges and universities elucidate the direction of the development of art thinking and politics in the future and strengthen the function of education. This study has been attempting to promote the major course of art thinking and politics for many years. In 2022, we collect a large number of students' evaluation data for this course using questionnaires. We sort the data, summarise them for mining and develope intelligent prediction models. Through the proposed bAMVO-KNN model, factors affecting students' overall evaluation of art ideology and politics course can be determined in the dataset, the most popular programmes can be summarised, the future trend can be judged and the potential correlation between factors can be analysed further to improve the content and form of art ideology and politics course to further strengthen the integration of ideology and politics and educate people through culture.

Nevertheless, this study has certain limitations that need to be examined: First, it is noteworthy that the samples used in this study

Table 7
Results of the Wilcoxon signed-rank test for the included methods.

Method		bWOA	bSAM	bHGS	bDE	bRUN	bMVO	bAMVO
Accuracy	Avg	4.5	4.05	4.1	3.65	4.6	3.8	3.3
	Rank	6	4	5	2	7	3	1
Sensitivity	Avg	3.8	4.1	4.15	3.8	3.8	4.55	3.8
	Rank	1	5	6	1	1	7	1
Specificity	Avg	4.55	4.25	3.85	3.7	4.7	3.65	3.3
	Rank	6	5	4	3	7	2	1
MCC	Avg	4.4	4.05	4.3	3.65	4.5	3.8	3.3
	Rank	6	4	5	2	7	3	1
Error	Avg	4.5	4.05	4.1	3.65	4.6	3.8	3.3
	Rank	6	4	5	2	7	3	1
Time cost	Avg	1	3.8	2.3	2.9	6.7	5.7	5.6
	Rank	1	4	2	3	7	6	5

Table 8
Detailed results obtained by the bAMVO-KNN model.

Fold	Selected feature subset size	ACC	Sensitivity	Specificity	MCC
#1	10	0.9843	1.0000	0.9672	0.9706
#2	11	0.9921	1.0000	0.9836	0.9849
#3	10	0.9921	1.0000	0.9836	0.9851
#4	9	1.0000	1.0000	1.0000	1.0000
#5	9	1.0000	1.0000	1.0000	1.0000
#6	10	1.0000	1.0000	1.0000	1.0000
#7	9	1.0000	1.0000	1.0000	1.0000
#8	9	1.0000	1.0000	1.0000	1.0000
#9	10	0.9921	1.0000	0.9836	0.9851
#10	7	1.0000	1.0000	1.0000	1.0000
Avg.	–	**0.9961**	**1.0000**	**0.9918**	**0.9926**
Std.	–	0.0056	0.0000	0.0116	0.0105

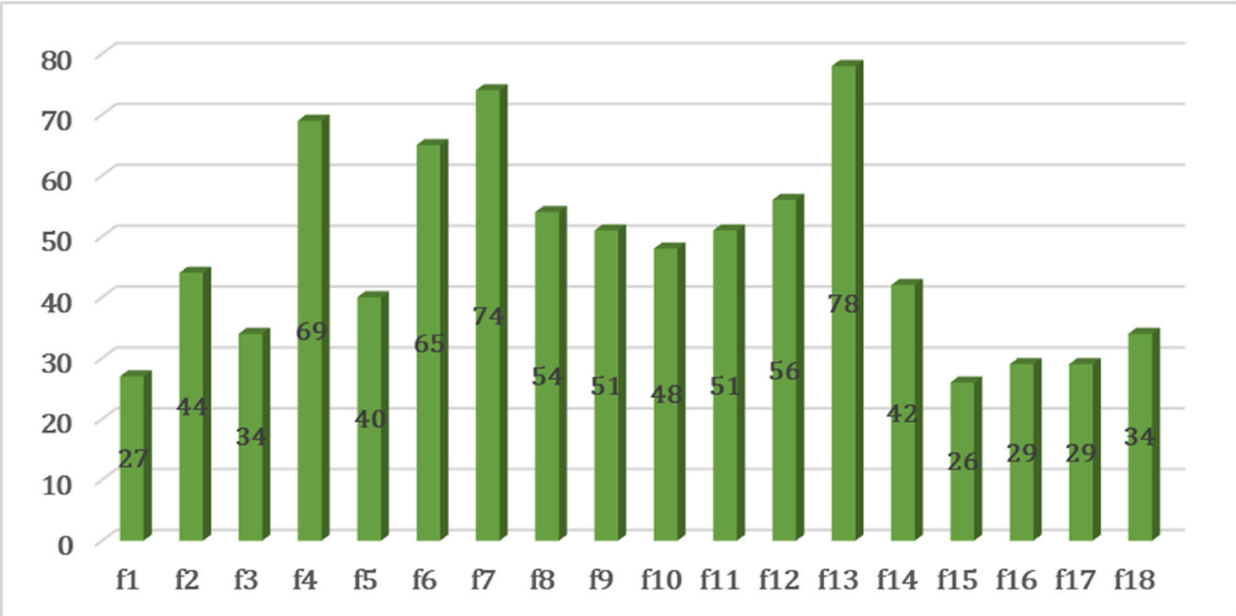

Fig. 6. Number of selected features obtained by the bAMVO-KNN model.

are of a restricted nature. To enhance the precision of the outcomes, it is important to gather a greater number of consecutive samples to train a learning model that is less prone to bias. Second, this study is only completed at one university, and it is imperative to undertake a multi-centre research approach to validate the findings. In addition, the boundaries of some questions in this study are slightly vague, and more attention should be paid to the objectivity of option collection. Ultimately, the number of criteria considered in this study is restricted, and it is recommended that future research endeavours identify more attributes that may considerably influence the comprehensive assessment of the ideological and political trajectories of art. To sum up, colleges and universities are fully exploiting the unique ideological and political education function of art, exploring the innovative path of art politicisation and ideological and political artistry, building an integrated education system of ‘art + ideological and political’, improving the teaching connotation with the reality of art, enriching educational practice with art and infiltrating the new generation with the beauty of art. Currently, there are primarily two approaches: theoretical and practical.

It is imperative to integrate beauty into teaching and create an excellent course in ‘art + politics’. We should pay attention to the organic integration of art courses and ideological and political education while promoting the coordinated education of professional courses as well as ideological and political education and achieving the ideological and political integration of art courses in every way. Furthermore, it is important to innovate the teaching reform of ‘one culture and six systems’ of ideological and political course, create golden ideological and political course, realise the innovation of the whole process of high-quality ideological and political course, promote 100 % coverage of ideological and political constructions of the curriculum, highlight humanistic and artistic feelings, strengthen the artistic education function of the ideological and political education of the curriculum and realise the promotion of ideological and political art of the curriculum in various fields.

In addition, it is necessary to transform beauty into practice and carry out the vivid practice of ‘art + politics’. First, the focus for activity education will be the second art classroom. Adhering to the educational function of campus culture, we meticulously construct campus cultural festivals, community cultural festivals and other signature events, fostering the integration of teachers and students, igniting campus creativity and embracing the aesthetics of life. Second, the platform of art creation integration is taken as the supporting point to achieve platform education. Through various art research platforms, education bases and entrepreneurial studios, students can feel the unique charm of art in innovation, creation and entrepreneurship. Finally, using the combination of artistic and cultural environments as a focal point, we aim to achieve environmental education. The school selects cultural venues, cultural landmarks and research hubs such as art, folk and specimen museums to achieve a complementary and mutually reinforcing relationship between art and technology.

6. Conclusion

This study proposes a machine learning model named AMVO-KNN as a means to achieve the core objective of developing morals and fostering individuals. To enhance the efficacy and robustness of the model, an ABC operator is incorporated into the MVO framework. The global optimality of the enhanced MVO is evaluated using a set of 23 benchmark functions. The experimental findings indicate that the algorithm proposed in this study exhibited superior performance in global optimisation over a range of test functions compared with seven alternative optimisation approaches. Similarly, a comparative analysis between bAMVO-KNN and the remaining six feature selection approaches reveale that the proposed model exhibite superior ACC and stability. The implementation of 10-fold CV trials is of utmost importance in understanding the interplay of art, science and technology.

To enhance the integration of art into ideological and political classes, colleges and universities are introducing courses that combine 'art ideological and political' with 'ideological and political as well as artistic form'. These courses aim to incorporate artistic ideological and political courses, adhere to aesthetic education and morality, cultivate people with virtue, integrate art aesthetic practice education into the ideological and political construction of colleges and universities, break through the long-term 'island effect' of ideological and political education supplemented by other professional education and give play to their own professional advantages. They also establish a long-term mechanism for coordinated development and education. However, students' evaluation of the major course of art thinking and politics has not been studied and it is difficult for colleges and universities to grasp the reform of art thinking and politics course. Therefore, it is important to conduct an in-depth analysis of the evaluation of college students' participation in the major courses of art thinking and politics, which will help colleges and universities elucidate the direction of the development of art thinking and politics in the future and strengthen the educational function of schools. This study collects many students' evaluation data for the course using questionnaires and establishes the bAMVO-KNN model. Through this model, we can identify the factors that affect students' overall evaluation of art thinking and politics in the dataset.

In the future, bAMVO can be used for other practical datasets and applied in more fields, including the assessment of parameters within photovoltaic systems [54,55], diagnostic processes for various diseases [56–58] and strategic formulation of the flight trajectories of unmanned aerial vehicles [59]. Finally, the introduced artificial prediction framework may well be anticipated to serve as a robust tool for a multitude of optimisation predicaments.

Data availability statement

Data will be made available on request.

Ethics statement

This study was approved by the Ethics Committee of the Communist Youth League of Wenzhou University, and the research conducted for this study did not require formal ethical approval given its nature. Because it did not directly involve the physiological, psychological and social risks and benefits of humans and animals.

CRediT authorship contribution statement

Xingzhong Zhuang: Writing - Original Draft, Writing - Review & Editing, Visualization, Formal analysis, Methodology. **Zhaodi Yi:** Software, Writing - Review & Editing, Visualization, Formal analysis, Methodology, Validation. **Yuqing Wang:** Methodology, Formal analysis, Data curation. **Yi Chen:** Investigation, Software, Writing - Original Draft, Writing - Review & Editing, Formal analysis, Methodology. **Sudan Yu:** Funding acquisition, Software, Formal analysis, Validation.

Declaration of competing interest

The authors declare that they have no known competing financial interests or personal relationships that could have appeared to influence the work reported in this paper.

Acknowledgements

A Project Supported by Scientific Research Fund of Zhejiang Provincial Education Department (No. Y202353056). This work was supported in part by National Social Science Foundation's research project on ideological and political courses in universities (No. 23VSZ087).

References

[1] X.Q. He, P.Y. Chen, J.T. Wu, Z. Dong, Deep learning-based teaching strategies of ideological and political courses under the background of educational psychology, Front. Psychol. 12 (2021). http://DOI:10.3389/fpsyg.2021.731166.
[2] D.B. Lu, Research-based teaching model of ideological and political course under computer network environment, Educ. Sci. Theor. Pract. 18 (5) (2018) 1784–1791. http://DOI:10.12738/estp.2018.5.078.
[3] N.B. Zhang, X.Q. Chen, H. Yin, Significance and possibility of VR technology embedded in the teaching of ideological and political theory course in colleges and universities, IEEE Access 8 (2020) 209835–209843. http://DOI:10.1109/ACCESS.2020.3023151.
[4] Y.J. Li, H. Mao, Study on machine learning applications in ideological and political education under the background of big data, Sci. Program. 2022 (2022), 3317876, http://DOI:10.1155/2022/3317876.
[5] L. Yin, H. Wang, S. Man, Y. Teng, X. Luo, Y. Li, [Ideological and political education in Microbiology Experiment: reform and exploration], Sheng wu gong cheng xue bao = Chinese journal of biotechnology 37 (4) (2021) 1434–1442. http://DOI:10.13345/j.cjb.200469.
[6] W. Si, L. Sun, Classification method of ideological and political resources of broadcasting and hosting professional courses based on SOM artificial neural network, Mobile Inf. Syst. (2022) 1–12, 2022, http://DOI:10.1155/2022/9220857.
[7] S. Li, H. Chen, M. Wang, A.A. Heidari, S. Mirjalili, Slime mould algorithm: a new method for stochastic optimization, Future Generat. Comput. Syst. 111 (2020) 300–323. http://DOI:10.1016/j.future.2020.03.055.
[8] A.A. Heidari, S. Mirjalili, H. Faris, I. Aljarah, M. Mafarja, H. Chen, Harris hawks optimization: algorithm and applications, Future Generation Computer Systems-the International Journal of Escience 97 (2019) 849–872. http://DOI:10.1016/j.future.2019.02.028.
[9] Y. Yang, H. Chen, A.A. Heidari, A.H. Gandomi, Hunger games search: visions, conception, implementation, deep analysis, perspectives, and towards performance shifts, Expert Syst. Appl. 177 (2021) 114864, https://doi.org/10.1016/j.eswa.2021.114864.
[10] J. Tu, H. Chen, M. Wang, A.H. Gandomi, The colony predation algorithm, JBE 18 (3) (2021) 674–710. http://DOI:10.1007/s42235-021-0050-y.
[11] I. Ahmadianfar, A. Asghar Heidari, A.H. Gandomi, X. Chu, H. Chen, RUN beyond the metaphor: an efficient optimization algorithm based on Runge Kutta method, Expert Syst. Appl. (2021) 115079, https://doi.org/10.1016/j.eswa.2021.115079.
[12] I. Ahmadianfar, A. Asghar Heidari, S. Noshadian, H. Chen, A.H. Gandomi, INFO: an efficient optimization algorithm based on weighted mean of vectors, Expert Syst. Appl. (2022) 116516, https://doi.org/10.1016/j.eswa.2022.116516.
[13] Q. Li, H. Chen, H. Huang, X. Zhao, Z. Cai, C. Tong, et al., An enhanced grey wolf optimization based feature selection wrapped kernel extreme learning machine for medical diagnosis, Comput. Math. Methods Med. 2017 (2017) 9512741. http://DOI:10.1155/2017/9512741.
[14] Z. Cai, J. Gu, C. Wen, D. Zhao, C. Huang, H. Huang, et al., An intelligent Parkinson's disease diagnostic system based on a chaotic bacterial foraging optimization enhanced fuzzy KNN approach, Comput. Math. Methods Med. 2018 (2018) 2396952. http://DOI:10.1155/2018/2396952.
[15] H. ling Chen, B. Yang, S. jing Wang, G. Wang, H. zhong Li, W. bin Liu, Towards an optimal support vector machine classifier using a parallel particle swarm optimization strategy, Appl. Math. Comput. 239 (2014) 180–197.
[16] W. Deng, X. Zhang, Y. Zhou, Y. Liu, X. Zhou, H. Chen, et al., An enhanced fast non-dominated solution sorting genetic algorithm for multi-objective problems, Inf. Sci. 585 (2022) 441–453, https://doi.org/10.1016/j.ins.2021.11.052.
[17] Y. Hua, Q. Liu, K. Hao, Y. Jin, A survey of evolutionary algorithms for multi-objective optimization problems with irregular Pareto fronts, IEEE/CAA Journal of Automatica Sinica 8 (2) (2021) 303–318.
[18] G. Hu, Y.X. Guo, G. Wei, L. Abualigah, Genghis Khan shark optimizer: a novel nature-inspired algorithm for engineering optimization, Adv. Eng. Inf. 58 (2023). http://DOI:10.1016/j.aei.2023.102210.
[19] M. Ghasemi, M. Zare, A. Zahedi, M.A. Akbari, S. Mirjalili, L. Abualigah, Geyser inspired algorithm: a new geological-inspired meta-heuristic for real-parameter and constrained engineering optimization, JOURNAL OF BIONIC ENGINEERING. 21 (1) (2023), 374-308, http://DOI:10.1007/s42235-023-00437-8.
[20] A.E. Ezugwu, J.O. Agushaka, L. Abualigah, S. Mirjalili, A.H. Gandomi, Prairie dog optimization algorithm, Neural Comput. Appl. 34 (22) (2022) 20017–20065. http://DOI:10.1007/s00521-022-07530-9.
[21] J.O. Agushaka, A.E. Ezugwu, L. Abualigah, Dwarf mongoose optimization algorithm, Comput. Methods Appl. Mech. Eng. 391 (2022). http://DOI:10.1016/j.cma.2022.114570.
[22] J.O. Agushaka, A.E. Ezugwu, L. Abualigah, Gazelle optimization algorithm: a novel nature-inspired metaheuristic optimizer, Neural Comput. Appl. 35 (5) (2023) 4099–4131. http://DOI:10.1007/s00521-022-07854-6.
[23] G. Hu, Y.X. Zheng, L. Abualigah, A.G. Hussien, DETDO: an adaptive hybrid dandelion optimizer for engineering optimization, Adv. Eng. Inf. 57 (2023). http://DOI:10.1016/j.aei.2023.102004.
[24] M. Zare, M. Ghasemi, A. Zahedi, K. Golalipour, S.K. Mohammadi, S. Mirjalili, et al., A global best-guided firefly algorithm for engineering problems, JOURNAL OF BIONIC ENGINEERING. 20 (5) (2023) 2359–2388. http://DOI:10.1007/s42235-023-00386-2.
[25] L. Abualigah, S. Ekinci, D. Izci, R.A. Zitar, Modified elite opposition-based artificial hummingbird algorithm for designing FOPID controlled cruise control system, Intelligent Automation & Soft Computing 0 (0) (2023) 1–10. http://DOI:10.32604/iasc.2023.040291.
[26] S. Wang, A. Zhou, G. Zhang, F. Fang, Learning regularity for evolutionary multiobjective search: a generative model-based approach, IEEE Comput. Intell. Mag. 18 (4) (2023) 29–42. http://DOI:10.1109/MCI.2023.3304080.
[27] Y. Chen, A. Zhou, Multiobjective portfolio optimization via Pareto front evolution, Complex & Intelligent Systems 8 (5) (2022) 4301–4317. http://DOI:10.1007/s40747-022-00715-8.
[28] H. Hao, X. Zhang, A. Zhou, Enhancing SAEAs with unevaluated solutions: a case study of relation model for expensive optimization, Sci. China Inf. Sci. 67 (2) (2024) 120103. http://DOI:10.1007/s11432-023-3909-x.
[29] J. Li, J. Lin, A probability distribution detection based hybrid ensemble QoS prediction approach, Inf. Sci. 519 (2020) 289–305, https://doi.org/10.1016/j.ins.2020.01.046.
[30] M.R. Chen, G.Q. Zeng, K.D. Lu, J. Weng, A two-layer nonlinear combination method for short-term wind speed prediction based on ELM, ENN, and LSTM, IEEE Internet Things J. 6 (4) (2019) 6997–7010. http://DOI:10.1109/JIOT.2019.2913176.
[31] X. Yang, D. Zhao, F. Yu, A.A. Heidari, Y. Bano, A. Ibrohimov, et al., An optimized machine learning framework for predicting intradialytic hypotension using indexes of chronic kidney disease-mineral and bone disorders, Comput. Biol. Med. 145 (2022) 105510. http://DOI:10.1016/j.compbiomed.2022.105510.
[32] X. Yang, D. Zhao, F. Yu, A.A. Heidari, Y. Bano, A. Ibrohimov, et al., Boosted machine learning model for predicting intradialytic hypotension using serum biomarkers of nutrition, Comput. Biol. Med. 147 (2022) 105752. http://DOI:10.1016/j.compbiomed.2022.105752.
[33] S. Mirjalili, S.M. Mirjalili, A. Hatamlou, Multi-Verse Optimizer: a nature-inspired algorithm for global optimization, Neural Comput. Appl. 27 (2) (2016) 495–513. http://DOI:10.1007/s00521-015-1870-7.
[34] X. Chen, H. Huang, A.A. Heidari, C. Sun, Y. Lv, W. Gui, et al., An efficient multilevel thresholding image segmentation method based on the slime mould algorithm with bee foraging mechanism: a real case with lupus nephritis images, Comput. Biol. Med. 142 (2022) 105179. http://DOI:10.1016/j.compbiomed.2021.105179.
[35] S. Jadhav, H.M. He, K. Jenkins, Information gain directed genetic algorithm wrapper feature selection for credit rating, Appl. Soft Comput. 69 (2018) 541–553. http://DOI:10.1016/j.asoc.2018.04.033.
[36] F, T., R. R, and A. R, Holdout validation for comparison classfication naïve bayes and KNN of recipient kartu Indonesia pintar, IOP Conf. Ser. Mater. Sci. Eng. 1125 (1) (2021).
[37] J. HoKun, Y. ChanSu, Enhancement of ship type classification from a combination of CNN and KNN, Electronics 10 (10) (2021).
[38] F. Zhu, X. Jia-kun, W. Zhong-yu, L. Pei-Chen, Q. Shu-jun, H. Lei, Image classification method based on improved KNN algorithm, J. Phys. Conf. 1930 (1) (2021).
[39] Y. Zhou, J. Xie, L. Li, M. Ma, Cloud model bat algorithm, Sci. World J. (2014) 237102. http://DOI:10.1155/2014/237102.
[40] D. Tian, J. Hu, Z. Sheng, Y. Wang, J. Ma, J. Wang, Swarm intelligence algorithm inspired by route choice behavior, JBE 13 (4) (2016) 669–678. http://DOI:10.1016/s1672-6529(16)60338-4.

[41] M. Mitić, N. Vuković, M. Petrović, Z. Miljković, Chaotic fruit fly optimization algorithm, Knowl. Base Syst. 89 (2015) 446–458. http://DOI:10.1016/j.knosys.2015.08.010.
[42] S. Mirjalili, SCA: a Sine Cosine Algorithm for solving optimization problems, Knowl. Base Syst. 96 (2016) 120–133. http://DOI:10.1016/j.knosys.2015.12.022.
[43] H. Chen, S. Jiao, A.A. Heidari, M. Wang, X. Chen, X. Zhao, An opposition-based sine cosine approach with local search for parameter estimation of photovoltaic models, Energy Convers. Manag. 195 (2019) 927–942.
[44] H. Chen, A.A. Heidari, X. Zhao, L. Zhang, H. Chen, Advanced orthogonal learning-driven multi-swarm sine cosine optimization: framework and case studies, Expert Syst. Appl. 144 (2020) 113113, https://doi.org/10.1016/j.eswa.2019.113113.
[45] S. Mirjalili, Moth-flame optimization algorithm: a novel nature-inspired heuristic paradigm, Knowl. Base Syst. 89 (2015) 228–249, https://doi.org/10.1016/j.knosys.2015.07.006.
[46] Y. Xu, H. Chen, J. Luo, Q. Zhang, S. Jiao, X. Zhang, Enhanced Moth-flame optimizer with mutation strategy for global optimization, Inf. Sci. 492 (2019) 181–203. http://DOI:10.1016/j.ins.2019.04.022.
[47] Y. Xu, H. Chen, A.A. Heidari, J. Luo, Q. Zhang, X. Zhao, et al., An efficient chaotic mutative moth-flame-inspired optimizer for global optimization tasks, Expert Syst. Appl. 129 (2019) 135–155, https://doi.org/10.1016/j.eswa.2019.03.043. http://DOI.
[48] S. García, A. Fernández, J. Luengo, F. Herrera, Advanced nonparametric tests for multiple comparisons in the design of experiments in computational intelligence and data mining: experimental analysis of power, Inf. Sci. 180 (10) (2010) 2044–2064. http://DOI:10.1016/j.ins.2009.12.010.
[49] J. Hu, W. Gui, A.A. Heidari, Z. Cai, G. Liang, H. Chen, et al., Dispersed foraging slime mould algorithm: continuous and binary variants for global optimization and wrapper-based feature selection, Knowl. Base Syst. 237 (2022). http://DOI:10.1016/j.knosys.2021.107761.
[50] W. Zhou, P. Wang, A.A. Heidari, X. Zhao, H. Chen, Spiral Gaussian mutation sine cosine algorithm: framework and comprehensive performance optimization, Expert Syst. Appl. 209 (2022). http://DOI:10.1016/j.eswa.2022.118372.
[51] S. Mirjalili, A. Lewis, The whale optimization algorithm, Adv. Eng. Software 95 (2016) 51–67, https://doi.org/10.1016/j.advengsoft.2016.01.008.
[52] R. Storn, K. Price, Differential evolution - a simple and efficient heuristic for global optimization over continuous spaces, J. Global Optim. 11 (4) (1997) 341–359. http://DOI:10.1023/A:1008202821328.
[53] E. Emary, H.M. Zawbaa, A.E. Hassanien, Binary grey wolf optimization approaches for feature selection, Neurocomputing 172 (2016) 371–381. http://DOI:10.1016/j.neucom.2015.06.083.
[54] S. Yu, A.A. Heidari, G. Liang, C. Chen, H. Chen, Q. Shao, Solar photovoltaic model parameter estimation based on orthogonally-adapted gradient-based optimization, Optik 252 (2022). http://DOI:10.1016/j.ijleo.2021.168513.
[55] S. Yu, A.A. Heidari, C. He, Z. Cai, M.M. Althobaiti, R.F. Mansour, et al., Parameter estimation of static solar photovoltaic models using Laplacian Nelder-Mead hunger games search, Sol. Energy 242 (2022) 79–104. http://DOI:10.1016/j.solener.2022.06.046.
[56] Z. Ullah, M. Jamjoom, Early detection and diagnosis of chronic kidney disease based on selected predominant features, Journal of healthcare engineering 2023 (2023) 3553216, 3553216, http://DOI:10.1155/2023/3553216.
[57] M.O. Karakus, O. Er, A comparative study on prediction of survival event of heart failure patients using machine learning algorithms, Neural Comput. Appl. 34 (16) (2022) 13895–13908. http://DOI:10.1007/s00521-022-07201-9.
[58] S. Lahmiri, Integrating convolutional neural networks, kNN, and Bayesian optimization for efficient diagnosis of Alzheimer's disease in magnetic resonance images, Biomed. Signal Process Control 80 (2023). http://DOI:10.1016/j.bspc.2022.104375.
[59] Y. Yu, H.L. Wang, S.M. Liu, L. Guo, P.L. Yeoh, B. Vucetic, et al., Distributed multi-agent target tracking: a nash-combined adaptive differential evolution method for uav systems, IEEE Trans. Veh. Technol. 70 (8) (2021) 8122–8133. http://DOI:10.1109/TVT.2021.3091575.